IEEE Open Journal of
Antennas and Propagation

Received 16 October 2023; accepted 3 November 2023. Date of publication 8 November 2023; date of current version 1 December 2023.

Digital Object Identifier 10.1109/OJAP.2023.3331217

Dispersion Characteristics and Applications of Higher Order Isosceles Triangular Meshes in the Finite Element Method

YUHUA NIU[1,2], JINBO LIU[1,2], WEN LUO[3], ZENGRUI LI[1,2] (Member, IEEE), AND JIMING SONG[1,2,4] (Fellow, IEEE)

[1] State Key Laboratory of Media Convergence and Communication, Communication University of China, Beijing 100024, China
[2] School of Information and Communication Engineering, Communication University of China, Beijing 100024, China
[3] School of Physics and Electronic Science, Guizhou Normal University, Guiyang 550025, China
[4] Department of Electrical and Computer Engineering, Iowa State University, Ames, IA 50011, USA

CORRESPONDING AUTHORS: J. LIU and J. SONG (e-mail: liuj@cuc.edu.cn; jisong@iastate.edu)

This work was supported in part by the National Natural Science Foundation of China under Grant 61971384 and Grant 62371427.

ABSTRACT Mesh division plays an important role in applications of the finite element method (FEM). The proposed research shows that under the same order, the equilateral triangular meshes have the most uniform dispersion distribution. The isosceles triangles with equal base and height have more uniform dispersion error than the square meshes, while the maximum phase error is similar. Taking the rectangular waveguide as an example, the relative errors in the cut-off frequency are analyzed based on different meshes. The numerical results show that under the same interpolation order and node numbers, the relative error of isosceles triangles with equal base and height for TE_{10} mode is the smallest. The results are useful in choosing appropriate element order, node density and mesh shape when applying FEM.

INDEX TERMS Dispersion error, equilateral triangular meshes, finite element method (FEM), isosceles triangular meshes, squares.

I. INTRODUCTION

With the rapid development of computer technology, the finite element method (FEM) is more and more widely used in solving electromagnetic problems. The solving process mainly includes four steps, i.e., region discretization, interpolation function selection, matrix equation establishment, and solution [1]. The FEM has nodal element-based and edge element-based schemes [2]. The advantage of the former one is simple for implementation and can be easily combined with various interpolation methods [3], while the advantage of the latter one is that it simplifies the application of boundary conditions [4], [5], [6].

In applications, the FEM has inherent error [7]. The main reason for this error is that the commonly used polynomial basis functions cannot accurately represent the field distribution in elements [2]. Because of this drawback, the plane wave cannot propagate through meshes with a fixed phase velocity, which will lead to numerical dispersion. Besides, the numerical dispersion is also related to incident wave direction, interpolation function order, mesh arrangement, etc. By studying the influence of these factors, it is helpful to understand the source of error in FEM [8].

Some scholars have studied the numerical dispersion in nodal elements of FEM. Platzman analyzed the simplest nodal element and noise sources in finite element solutions for tidal models [9]. The one-dimensional high order case is studied in [10], which shows that high order elements can significantly reduce the discretization error. Mullen and Belytschko studied the numerical dispersion of plane waves, which propagates through the first order periodic meshes composed of triangular and quadrilateral elements [11]. It was found that the dispersion error depends on the wave propagation direction. Lynch et al. worked on FEM errors in hyperthermia applications and demonstrated the influence of lossy materials on errors [12]. Warren and Scott focused on numerical dispersion of two-dimensional (2D) nodal

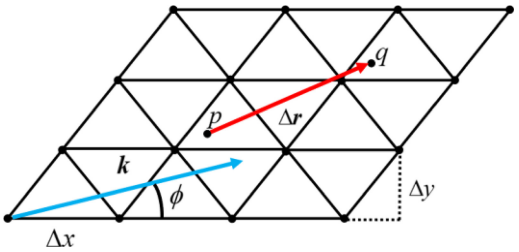

FIGURE 1. Schematic diagram of plane wave propagation in 2D uniform finite element meshes.

methods [8], whose research greatly expanded the nodal element dispersion analysis.

Interpolation methods based on different meshes have different errors. Luo et al. found the advantage of triangular interpolation method by selecting the interpolation region with less error. Compared with the traditional interpolation based on rectangular meshes, the right triangular interpolation method is more effective, and the equilateral triangular interpolation method is more accurate [13], [14].

Recently, Liu et al. proposed an improved method based on non-uniform isosceles triangular interpolation to accelerate the solution of multilevel fast multipole algorithm (MLFMA) [15]. Compared with the Lagrange method, this method uses fewer sampling points and can reduce the operation time without affecting the accuracy. In [16], the isosceles triangular meshes in the FEM are analyzed. The phase error distributions of the first and second order FEM over isosceles triangles are given. The innovation of this paper is to expand the error analysis on the basis of [16] with more details, the root mean square (RMS) errors of different meshes are analyzed, and the extension to the third order in the error analysis. Taking the calculation of the cut-off frequency of the rectangular waveguide as an example, it is found that the isosceles triangle with the same base and height has the smallest relative error in the dominant mode TE_{10}. Relevant results can be used to select the appropriate FEM mesh and interpolation order, by analyzing the dispersion errors of isosceles triangles with different proportions of height and base, it can also provide theoretical support for adaptive mesh generation.

II. DISPERSION THEORY

Considering a plane wave propagating at any direction in 2D periodic elements, the field in the element can be represented by a discrete Helmholtz equation [8]. The field between point p in one element and point q in another element at the corresponding position has a simple phase relationship, where $\Delta\mathbf{r}$ is the distance vector between these two points, as shown in Fig. 1.

To describe the accuracy of nodal element, the phase error in degree for a wave propagating in one wavelength is expressed as [8]

$$\delta = 360\left|\frac{\bar{k}-k}{k}\right| \tag{1}$$

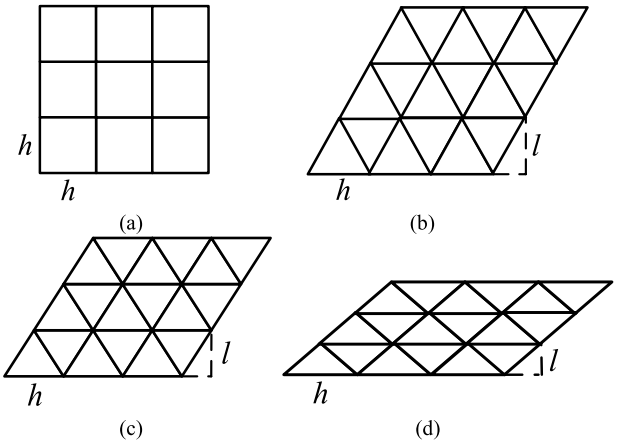

FIGURE 2. Schematic diagram of different mesh arrangements in 2D plane, (a) Square meshes, (b) Isosceles triangular meshes $l = h$, (c) Equilateral triangular meshes, (d) Isosceles triangular meshes $l = 0.5h$.

Considering the periodicity of mesh arrangements, it is necessary to select appropriate regions of interest, which will ensure the integrity of equations. Next, interpolation functions of different orders are selected. When the mesh shape and interpolation order are determined, the actual sampling points used for interpolation are found. For the calculation of specific matrix elements, the first and second orders can use the existing analytical formula [1]. However, the formula substitution of the third order elements is very complicated, so the Gauss-Legendre numerical integration is introduced for the numerical integration. Taking the triangular element as an example, the numerical integration is expressed as [1]

$$\iint_{\Omega^e} F\left(L_1^e, L_2^e, L_3^e\right)dxdy = \Delta^e \sum_{i=1}^{m} W_i F\left(L_{1i}^e, L_{2i}^e, L_{3i}^e\right) \tag{2}$$

where m is the number of sampling points, Δ^e is the area of the element, $(L_{1i}^e, L_{2i}^e, L_{3i}^e)$ are functions of sampling point (x, y), and W_i is the weighting factor of each sampling point for the numerical integral. The number of unknowns and independent equations are determined by the simple phase relationship between nodes. Then, the coefficient matrix in FEM is obtained. Finally, the numerical wave number can be solved when the determinant of the coefficient matrix is zero.

III. NUMERICAL DISPERSION ERRORS AND ANALYSIS

Taking the first order elements as examples, the different meshes investigated in this paper are shown in Fig. 2. In the higher order elements, the sampling interval between nodes remains constant, while more sampling points begin to appear at the edges and inside of the element.

As shown in Fig. 3, the phase errors of each mesh vary with wave propagation directions. For equilateral triangles, the dispersion error distribution is the smallest and the most uniform, because the error term in the third order Taylor

TABLE 1. The Max error, RMS error, and their ratio corresponding to first order elements with $\lambda/h = 10$.

Mesh	Max error	RMS error	Max/RMS
$l = 0.5h$	7.044	4.118	1.702
$l = \sqrt{3}h/2$	4.308	4.303	1.002
$l = h$	5.673	5.074	1.118
square	5.670	4.403	1.288

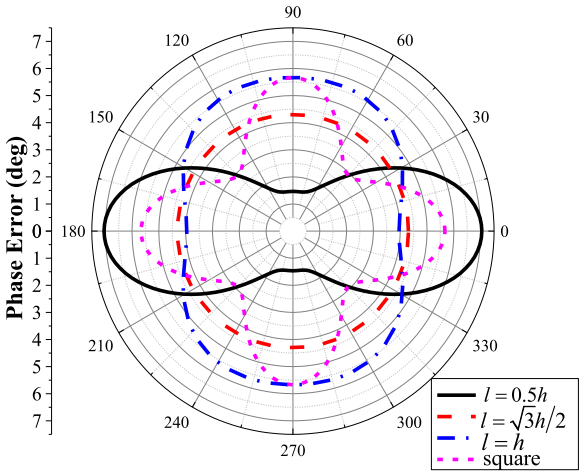

FIGURE 3. The phase error in degree per wavelength for the first order elements with different meshes, the error is a function of Φ with $\lambda/h = 10$.

expansion does not depend on the angle Φ, the formula is expressed as [17]

$$\bar{k} = k\left(1 - \frac{k^2h^2}{32}\right) \tag{3}$$

Quantitative analysis can be further done by the data in Table 1. RMS error in the table is used to measure the overall error. The ratio of maximum error to RMS error can be used to characterize the anisotropy of dispersion. Obviously, equilateral triangles have the smallest error ratio. The dispersion error of isosceles triangles with $l = h$ is also relatively uniform. and maximum phase error is close to square meshes. For isosceles triangles with $l = 0.5h$ and squares, the maximum phase errors drastically change with the directions. It is observed that squares have the largest phase error when $\Phi = 0°$, $90°$, $180°$, and $270°$, because only two of the four interpolation points are used. The isosceles triangles with $l = 0.5h$ have the largest error at $\Phi = 0°$ and $\Phi = 180°$, and the smallest error at $\Phi = 90°$ and $\Phi = 270°$. It is simply due to the vertical sampling interval is smaller than the horizontal sampling interval.

Dispersion error distributions with the second order interpolation elements are shown in Fig. 4. It can be found that the maximum phase error of equilateral triangular meshes is more irregular than the first order, and the error anisotropy is more obvious. However, compared with other meshes of the same order, the equilateral triangles still have the most uniform dispersion error. The isosceles triangles with $l = h$ has more uniform error distribution than squares, and from the second order, the maximum phase error of the former

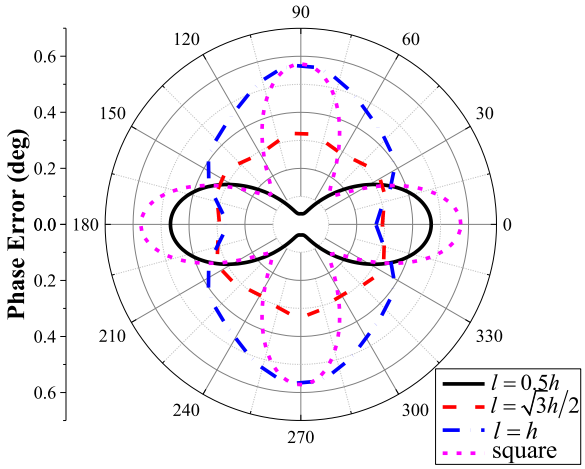

FIGURE 4. The phase error in degree per wavelength for the second order elements with different meshes, the error is a function of Φ with $\lambda/h = 10$.

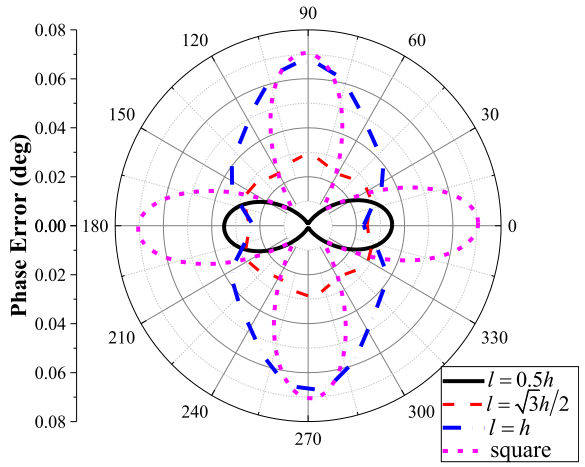

FIGURE 5. The phase error in degree per wavelength for the third order elements with different meshes, the error is a function of Φ with $\lambda/h = 10$.

starts to be smaller than the later. It is observed in Table 2 that the maximum error of equilateral triangular meshes is the smallest, and the error ratio is also the smallest. The maximum dispersion error of squares is the largest. The error ratio of isosceles triangle with $l = h$ is smaller than that of squares. The error ratio of isosceles triangles with $l = 0.5h$ is the largest, while the anisotropy is the strongest.

For the third order interpolation, the phase errors for different meshes are functions of wave propagation directions, as shown in Fig. 5. It is found that the higher interpolation order is, the smaller dispersion error is. The dispersion distributions are similar with lower orders. At the same time, with the increase of the order, the error ratios of four meshes also gradually increases. The data from Table 3 support this conclusion.

In order to more fairly compare the maximum dispersion errors of different meshes when the number of sampling points increases, λ^2/S is defined as the sampling density, S is the area occupied by each sampling point [16]. Particularly,

TABLE 2. The Max error, RMS error, and their ratio corresponding to second order elements with $\lambda/h = 10$.

Mesh	Max error	RMS error	Max/RMS
$l = 0.5h$	0.467	0.255	1.832
$l = \sqrt{3}h/2$	0.326	0.309	1.055
$l = h$	0.567	0.433	1.309
square	0.572	0.392	1.462

TABLE 3. The Max error, RMS error, and their ratio corresponding to third order elements with λ/h=10.

Mesh	Max error	RMS error	Max/RMS
$l = 0.5h$	0.035	0.018	1.902
$l = \sqrt{3}h/2$	0.029	0.027	1.079
$l = h$	0.067	0.045	1.474
square	0.071	0.045	1.577

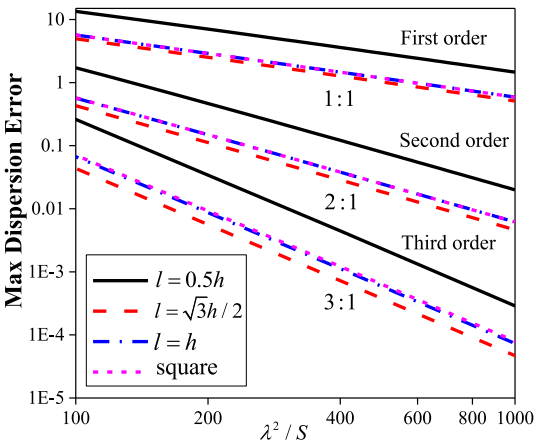

FIGURE 6. The maximum dispersion error in degree per wavelength for different orders of elements, the error is as a function of λ^2/S.

$S = hl$ is for isosceles triangular meshes and $S = h^2$ is for square meshes, the reason is that square vertices share with four neighboring elements, and triangular vertices share with six neighboring elements. It is indicated in Fig. 6 that higher order elements dramatically decrease the phase error. It is found that the maximum dispersion error of equilateral triangles is the smallest under the same order. The maximum dispersion error of isosceles triangles with $l = h$ is similar to the squares, and the error of isosceles triangles with $l = 0.5h$ is the largest. Further research shows that the error decrease slope is corresponding to the interpolation function order. For the first order interpolation, the slope of error curve is 1, and for the second and third order cases, the slope is 2 and 3, respectively.

IV. APPLICATION IN CALCULATION OF CUTOFF FREQUENCY

In order to further illustrate the difference of different FEM meshes in solving specific engineering problems, the calculation of the cutoff frequency of a rectangular waveguide is selected as an example. The numerical cutoff frequencies are obtained by using different FEM meshes for the same cross section. Because of the complexity of implementing the third order meshes in FEM calculation of the cut-off frequency, the analysis takes the first and second order meshes as examples.

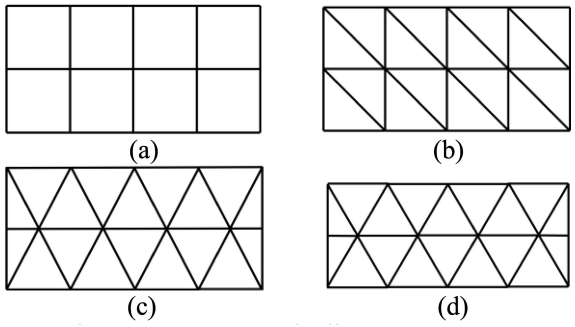

FIGURE 7. Schematic diagram of different mesh arrangement in rectangular waveguide. (a) Square meshes, (b) Isosceles right triangular meshes, (c) Isosceles triangular meshes $l = h$, (d) Equilateral triangular meshes.

It is assumed that the long side $a = 2$ cm and the short side $b = 1$ cm of the rectangular waveguide. Considering a fair mesh comparison, it is necessary to use the same sampling density λ^2/S for dominant meshes. For example, when the mesh is a square, the long side of the waveguide is divided into 20 segments, and the short side is divided into 10 segments, a total of 20×10 small square meshes. When using isosceles triangular meshes $l = h$, because it has the same S with square, it is also divided into 20 and 10 segments. It's important to note that in addition to the isosceles triangles with $l = h$, there are also right triangles along the short edges. Let the radius of the inscribed circle of a triangle be r and the radius of the circumscribed circle be R. For isosceles triangular meshes $l = h$, $2r/R = 0.989$. For right triangles at the corner, $2r/R = 0.683$. When using equilateral triangles, keep S similar to the above meshes. The long side is divided into 18 segments and the short side is divided into 10 segments. There are right triangles along the short edges too. In near equilateral triangle meshes, $2r/R = 0.999$ in most parts, and $2r/R = 0.720$ for the right triangles. For isosceles right triangle meshes, to keep the same S, the long side is divided into 20 segments and the short side into 10 segments. The simplified mesh arrangements are shown in Fig. 7.

The most used mode in the rectangular waveguide is the dominant mode TE_{10}. Taking dominant mode as an example, relative errors in cutoff frequency with four meshes are analyzed. When the meshes become finer and finer, the right triangles along the short edges become less and less important to meshes of isosceles triangles with $l = h$ and equilateral triangular meshes. As shown in Fig. 8, for the first order, the relative error of isosceles triangular meshes $l = h$ is the smallest under the same number of sampling points. The errors of right triangles and squares are the largest. The reason for partial bending of the curve of the equilateral triangle is that not all triangles shown in Figure 7(d) are exactly equilateral. The right triangles appearing at the corners of the mesh would further introduce errors. The shape of dominant meshes under different number segments

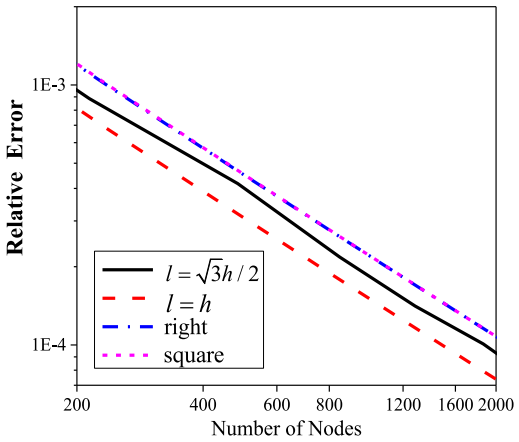

FIGURE 8. The relative errors in cutoff frequency for the first order different meshes with the number of sampling points. "square" refers to the mesh (a), "right" to (b), "$l = h$" to (c), and "$l = \sqrt{3}h/2$" to (d) as shown in Fig. 7.

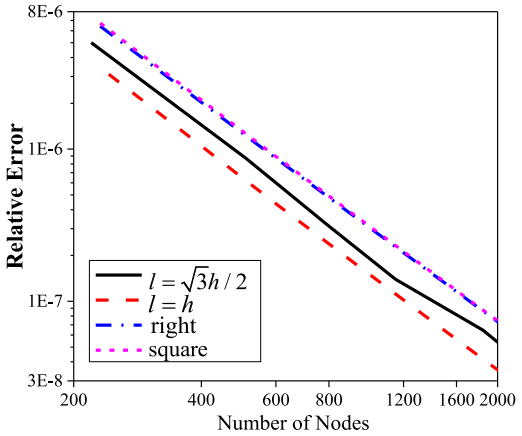

FIGURE 9. The relative errors in cutoff frequency for the second order different meshes with the number of sampling points. "square" refers to the mesh (a), "right" to (b), "$l = h$" to (c), and "$l = \sqrt{3}h/2$" to (d) as shown in Fig. 7.

TABLE 4. The relation between l/h of the first order near equilateral triangular meshes and the numbers of segments along the long and short sides.

(N_x,N_y)	(9,5)	(27,16)	(46,26)	(65,37)	(83,48)
l/*h*	0.900	0.844	0.885	0.878	0.865

TABLE 5. The relation between l/h of the second order near equilateral triangular meshes and the numbers of segments along the long and short sides.

(Nx,Ny)	(9,5)	(18,10)	(27,16)	(37,21)	(46,26)
l/*h*	0.900	0.900	0.844	0.881	0.885

is shown in Table 4. For second order meshes, the same conclusion can be obtained from Fig. 9 and the shape data of near equilateral triangles is illustrated in Table 5.

V. CONCLUSION

The plane wave has different dispersion properties when passing through different meshes of FEM. The square mesh based on Lagrange interpolation is used to compare with the proposed meshes. Under the same interpolation order and sampling density, dispersion error of isosceles triangular meshes $l = h$ is more uniform than square meshes. Starting from the second order interpolation, the maximum dispersion error of isosceles triangles with $l = h$ is smaller than that of square meshes. The dispersion error of equilateral triangular meshes is the most uniform. The higher the order is, the faster the maximum dispersion error decrease. The calculation of cutoff frequency of the rectangular waveguide shows that under the same order, the relative error of isosceles triangular meshes $l = h$ for TE_{10} mode is the smallest.

REFERENCES

[1] J. M. Jin, *The Finite Element Method in Electromagnetics*. 2nd. ed. Hoboken, NJ, USA: Wiley, 2002.

[2] G. S. Warren and W. R. Scott, "An investigation of numerical dispersion in the vector finite element method using quadrilateral elements," *IEEE Trans. Antennas Propag.*, vol. 42, no. 11, pp. 1502–1508, Nov. 1994.

[3] W. E. Boyse and K. D. Paulsen, "Accurate solutions of Maxwell's equations around PEC corners and highly curved surfaces using nodal finite elements," *IEEE Trans. Antennas Propag.*, vol. 45, no. 12, pp. 1758–1767, Dec. 1997.

[4] A. F. Peterson, "Vector finite element formulation for scattering from two-dimensional heterogeneous bodies," *IEEE Trans. Antennas Propag.*, vol. 43, no. 3, pp. 357–365, Mar. 1994.

[5] T. V. Yioultsis and T. D. Tsiboukis, "Multiparametric vector finite elements: A systematic approach to the construction of three-dimensional, higher order, tangential vector shape functions," *IEEE Trans. Mag.*, vol. 32, no. 3, pp. 1389–1392, Jun. 1996.

[6] T. Mifune, S. Isozaki, T. Iwashita, and M. Shimasaki, "Algebraic multigrid preconditioning for 3-D magnetic finite-element analyses using nodal elements and edge elements," *IEEE Trans. Mag.*, vol. 42, no. 4, pp. 635–638, Apr. 2006.

[7] R. Lee and A. C. Cangellaris, "A study of discretization error in the finite element approximation of wave solutions," *IEEE Trans. Antennas Propag.*, vol. 40, no. 5, pp. 542–549, May 1992.

[8] G. S. Warren and W. R. Scott, "Numerical dispersion of higher order nodal elements in the finite-element method," *IEEE Trans. Antennas Propag.*, vol. 44, no. 3, pp. 317–320, Mar. 1996.

[9] G. W. Platzman, "Some response characteristics of finite-element tidal modes," *J. Comput. Phys.*, vol. 40, pp. 36–63, Mar. 1981.

[10] W. R. Scott, " Errors due to spatial discretization and numerical precision in the finite-element method," *IEEE Trans. Antennas Propag.*, vol. 42, no. 11, pp. 1565–1570, Nov. 1994.

[11] R. Mullen and T. Belytschko, "Dispersion analysis of finite element semidiscretizations of the two-dimensional wave equation," *Int. J. Numer. Methods Eng.*, vol 18, pp. 11–29, Jan. 1982.

[12] D. R. Lynch, K. D. Paulsen, and J. W. Strohbehn, "Finite element solution of Maxwell's equations for hyperthermia treatment planning," *J. Comput. Phys.*, vol. 58, pp. 246–269, Apr. 1985.

[13] W. Luo, J. Liu, Z. Li, and J. Song, "Efficient triangular interpolation methods: Error analysis and applications," *IEEE Antennas Wireless Propag. Lett.*, vol. 19, no. 6, pp. 1032–1036, Jun. 2020.

[14] W. Luo, J. Liu, Z. Li, and J. Song, "Error analysis of higher order bivariate Lagrange and triangular interpolations in electromagnetics," *IEEE Open J. Antennas Propag.*, vol. 1, pp. 590–597, 2020.

[15] J. Liu, W. Luo, J. Song, and Z. Li, "Improving the efficiency of three-dimensional multilevel fast multipole algorithm by the triangular interpolation," *IEEE Trans. Antennas Propag.*, vol. 71, no. 2, pp. 1697–1705, Feb. 2023.

[16] Y. Niu, J. Liu, W. Luo, and J. Song, "Numerical dispersion analysis of isosceles triangular meshes in the finite-element method," in *Proc. Int. Appl. Comput. Electrom. Soc. Symp. (ACES-China)*, 2022, pp. 1–2.

[17] Y. Niu, "Dispersion and applications of meshes based on nodal element in the finite element method," M.S. thesis, Commun., Univ. of China, Beijing, China, 2023.